

Neutron thermal cross sections of 3D-printing organic polymers using the Average Functional Group Approximation

Giovanni Romanelli^{1,2*}, Margherita Simoni¹, Enrico Preziosi^{1,2}, Jose Ignacio Marquez Damian³, Carla Andreani^{1,2,4}, and Roberto Senesi^{1,2}

¹Physics Department, Università degli Studi di Roma “Tor Vergata”, via della Ricerca Scientifica 1, 00133, Roma, Italy

²NAST Centre, Università degli Studi di Roma “Tor Vergata”, via della Ricerca Scientifica 1, 00133, Roma, Italy

³European Spallation Source ERIC, PO Box 176, 22100 Lund, Sweden

⁴Istituto IPCP-CNR, Viale J.F. Kennedy 54, 80125 Naples, Italy

Abstract. We provide a worked example on how to obtain the total neutron scattering cross section of organic polymers at thermal neutron energies by means of the Average Functional Group Approximation. Within this framework, a polymer is rationalised as composed of hydrogen atoms belonging to specific functional groups, therefore taking into account the material-specific incoherent inelastic scattering contributions to the thermal cross section. Such simplified model allows the calculation of thermal neutron cross sections for a broad variety of materials of interest in neutron applications, *e.g.*, sample containers and shielding components. We discuss in detail the case of ABS, often available as a 3D-printing material, whereby three polymers (acrylonitrile, butadiene, and styrene) can be combined in several mass percentages depending on the final application. Results are obtained using the NCrystal module already featuring the Average Functional Group Approximation.

1 Introduction

Thermal neutron Cross Sections (TCSs) of hydrogenous materials are a fundamental ingredient for the simulation and design of, amongst other things, nuclear reactors, neutron moderators, shielding materials, phantoms for radiation protection and for the transport codes employed in neutron capture therapy. However, experimental TCSs are available for just a handful of materials (see, *e.g.*, Ref. [1]). In order to match the level of detail in modern Monte Carlo nuclear transport codes, the possibility to calculate TCSs from simplified models, molecular dynamics, and *ab initio* calculations has been a topic of recent development (see, *e.g.*, Refs. [2–11]).

Within this framework, the Average Functional Group Approximation (AFGA) [12] was developed as a simplified phenomenological approach for the accurate calculation of TCSs of large organic molecules and polymers. While using only a limited number of effective Vibrational Densities of States (VDoSs), representing the hydrogen dynamics of functional groups within organic molecules, the model allows an accurate prediction, within the incoherent approximation, of the total cross sections from a vast series of polymers. The model was developed based on neutron transmission measurements at the VESUVIO spectrometer of the ISIS Neutron and Muon Source [13–16] to determine the total neutron cross section of all proteinogenic amino acids. Each molecular system was simulated using phonon calculations, and the hydrogen-projected VDoSs within different functional groups in the

molecule was isolated. For each functional group, VDoSs were averaged over all amino acids containing them [12]. This procedure effectively takes into account the variety of local environments of each functional group in large organic systems, therefore proving particularly suitable for macromolecules and polymers. Such large systems, whose modelling with atomistic simulations is prohibitively challenging, can be simply rationalised in the AFGA as a combination of contributions from average functional groups.

Here, we discuss the application of AFGA to materials used for 3D printing, as a further example beyond those already available in the literature [17, 18]. For some of these materials, a number of different recipes exist where monomers and small polymer chains are combined with different stoichiometries and, therefore, represent an unlimited and interesting class of materials for which AFGA can provide a game-changing approach.

2 Materials and Methods

The total scattering cross section, as a function of the incident neutron energy E , is obtained by integration over all the values of the final neutron energy E' and scattering angle, Ω , as

$$\sigma_s(E) = \int dE' \int d\Omega \frac{d^2\sigma}{dE'd\Omega} \quad (1)$$

where the double differential cross section can be related to the dynamic structure factor [19], $S(Q, \omega)$, dependent on the neutron energy ($\hbar\omega$) and wavevector (Q) transfers

*e-mail: giovanni.romanelli@uniroma2.it

in the scattering event, and takes into account any elastic and inelastic, coherent and incoherent process. Within the incoherent approximation, particularly suitable to describe hydrogen-rich materials such as organic compounds and polymers, the dynamic structure factor largely simplifies [19], and can be expressed as

$$\frac{d^2\sigma}{dE'd\Omega} = \sqrt{\frac{E'}{E}} \sum_i N_i \frac{\sigma_{b,i}}{4\pi} S_i(Q, \omega) \quad (2)$$

where the sum runs over all the isotopes i within the sample, each corresponding to N_i scattering centres. The total cross section, also including the absorption contribution $\sigma_a = \sum_i N_i \sigma_{a,i}$, is defined as

$$\sigma(E) = \sigma_s(E) + \sigma_a \sqrt{\frac{E_0}{E}}, \quad (3)$$

where the isotope-specific absorption cross section $\sigma_{a,i}$ (at the reference energy of $E_0 = 25.3$ meV) and bound scattering cross sections, $\sigma_{b,i}$, are energy-independent tabulated values [20].

Calculations of $\sigma_s(E)$ for several polymers used as 3D printing materials were based on the formalism developed in Ref. [12] and run within the NCrystal environment [21]. In particular, polymers were rationalised based on their functional groups, as reported in Table 1, particularly based on their aromatic, aliphatic methine, methylene, methyl, amine and hydroxyl groups. NCrystal already features polylactic acid, polycarbonate, polypropylene and other polymers having made use of the AFGA approach (see Ref. [22]). The TCSs for additional materials, in particular acrylonitrile, butadiene and styrene, were calculated here as the main ingredients for ABS, whose chemical structure is the one schematically reported in Figure 1, with acrylonitrile, butadiene, and styrene repeated x , y , and z times, respectively. As an example, we show below the code to obtain acrylonitrile from NCrystal using the AFGA approach.

```
# create material in NCrystal
# using the AFGA model
!ncrystal_hfg2ncmat --formula C3H3N
--spec 1xCHali+1xCH2
--density 0.81
--title acrylonitrile
-o acrylonitrile.ncmat

T = '300K' # Temperature in K
fn = 'acrylonitrile.ncmat;temp='+T
pc = NC.createScatter(fn)
# calculate absorption cross section
absorption = NC.createAbsorption(fn)
xs_abs = absorption.crossSectionNonOriented(E)
# calculate scattering cross section
xs = pc.crossSectionNonOriented(E)
```

3 Results and Discussion

The total scattering cross section, $\sigma_s(E)$ per formula unit (*i.e.*, per chemically and stoichiometrically defined fundamental molecular component) and linear scattering attenuation factor per mass unit, $\Sigma_s(E)/\rho$, were calculated for acrylonitrile, butadiene and styrene. In a good-geometry

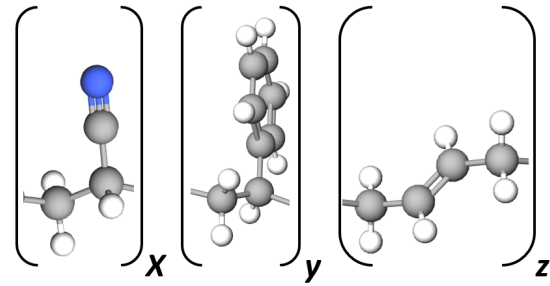


Figure 1. Schematic representation of the ABS polymer based on its unit constituents: acrylonitrile (repeated x times), butadiene (repeated y times) and styrene (repeated z times).

transmission experiment, by using the Beer-Lambert law, one can express the transmission as a function of the incident neutron energy, $T(E)$, as

$$T(E) = \exp\left(-\sum_k n_k \sigma_k(E) d\right) = \exp\left[-\rho \left(\frac{\Sigma(E)}{\rho}\right) d\right], \quad (4)$$

where the sum runs over the materials within the sample under consideration, and the mass attenuation cross section can be obtained from the ones of its constituent polymers, weighted by their mass percentages, as

$$\left(\frac{\Sigma(E)}{\rho}\right) = \sum_k \frac{\rho_k}{\rho} \left(\frac{\Sigma(E)}{\rho}\right)_k = \sum_k \frac{\rho_k}{\rho} \left(\frac{\sigma_k(E) N_A}{M_k}\right), \quad (5)$$

with N_A the Avogadro's constant and m_k the mass of the molecule per formula unit. Finally, n_k and ρ_k are the number density and mass density of compound k , respectively, and ρ is the mass density of the sample.

Results for the three polymers are reported in Figure 2, showing the total scattering cross section (top) and the mass attenuation coefficient (bottom panel). Both functions were calculated at the two temperatures of 10 K (filled markers), as an example of base temperature where all vibrational modes are frozen in their ground state, and 300 K (empty markers), as an example of room temperature where each mode is populated based on the Maxwell Boltzmann statistics.

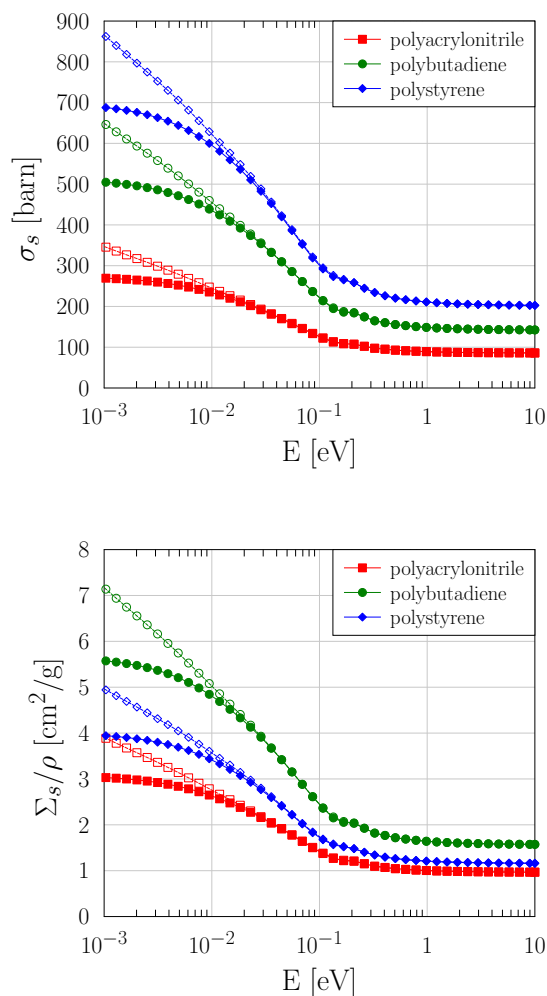
As one can appreciate from Figure 2, in the incoherent approximation, the energy-dependent total scattering cross section per formula unit has two simple limits. On the one side, at neutron energies lower than few meV and at base temperatures, one has $\sigma_s(E) = \sum_i N_i \sigma_{b,i}$. This stops to be the case at higher temperatures, already at tens of K, as inelastic scattering events where the neutron gains energy from the low-energy lattice and molecular vibrations start to play a role. On the other side, at epithermal energies larger than few eV, at any temperature of the system, one has $\sigma_s(E) = \sum_i N_i \sigma_{f,i}$, where the free scattering cross section of each isotope is defined as

$$\sigma_{f,i} = \frac{\sigma_{b,i}}{(1 + m_N/m_i)^2}, \quad (6)$$

and where m_N and m_i are the masses of the neutron and the isotope, respectively. It is worth noting that for hydrogen

Table 1. Rationalisation of organic polymers based on their hydrogen-containing functional groups. The density and molecular mass per formula unit for each material are also reported.

Material	Formula	CH_3	CH_2	CH_{ali}	Other	Mass (a.m.u.)	Density (g/cm^3)
Polylactic acid	$(C_3H_4O_2)_n$	1	–	1	–	72.06	1.43
Polycarbonate	$(C_{16}H_{14}O_4)_n$	2	–	–	$8CH_{aro}$	272.29	1.20
Polypropylene	$(C_3H_6)_n$	1	1	1	–	42.08	0.90
Acrylonitrile	$(C_3H_3N)_n$	–	1	1	–	53.06	0.81
Butadiene	$(C_4H_6)_n$	–	2	2	–	54.09	0.61
Styrene	$(C_8H_8)_n$	–	1	1	$5CH_{aro}$	104.15	0.91
PAPP	$(C_4H_{10}N_2H_4O_7P_2)_n$	–	4	–	$2OH, 2NH_2$	264.11	1.50

**Figure 2.** The total scattering cross section per monomer unit (top) and mass attenuation coefficient (bottom) for the acrylonitrile (red squares), butadiene (green circles) and styrene (blue diamonds) polymers. The reported spectra take into account scattering contributions only (absorption cross sections not included). Filled and empty markers refer to 10 K and 300 K, respectively.

($m_H = 1$) the free and bound scattering cross sections differ by approximately a factor of 4, while such difference becomes increasingly negligible as the isotope's mass increases. At any intermediate energy, and any temperature above few K, the total scattering cross section becomes

a function of the temperature and changes depending on the structure and dynamics of the molecular system under consideration, and the correspondence with single-particle contributions becomes more difficult to evaluate, as one needs to consider each isotope-projected VDoS and a full multi-phonon expansion. Moreover, considering the similarity between bound and free cross sections for elements heavier than hydrogen, as well as the lower absolute values of their bound scattering cross sections, the contributions to the scattering cross section from N, C and O in the AFGA model are only proportional to their free cross sections and stoichiometry over the entire energy range considered.

Having defined the mass attenuation coefficients for the main ingredients of ABS polymers, we used this information to predict the total mass attenuation coefficient of an ABS compound for a given recipe (see Ref. [23]) considering 7.1 wt% acrylonitrile, 12.9 wt% butadiene, and 80 wt% styrene. The result, calculated at 300 K and labelled as ABS in the Figure 3, is compared with polystyrene, as this is the main component by mass. It is worth noting that, while in a traditional *ab initio* approach one should calculate a VDoS related to the typical recipe-specific ABS compound (over a very large crystal unit cell to take into account polymer length and disorder), the AFGA approach allows to calculate the attenuation coefficient of the compound as a simple linear combination of the constituent polymers. This is expected to be an accurate representation of the TCS of the system as long as the molecular system is composed of a large number of atoms (always true for polymers), owing to the average nature of the VDoSs of each functional group defined in the AFGA framework. This is an additional proof of the central limit theorem for the hydrogen nuclear dynamics [24].

To complete this worked example on the use of AFGA, we extend the calculations presented in Figure 3 to the case discussed in Ref. [23], where ABS was mixed with piperazine pyrophosphate (PAPP, see Table 1) a flame-retardant reducing the risks associated to ABS ignition. Following the same rationalisation discussed above, we have calculated the mass attenuation coefficient of PAPP (dashed line in Figure 3), and calculated the same function for a copolymer made of 25 wt% PAPP and 75 wt% ABS. The result is displayed as a dotted-dashed line in the same figure. One can notice how, using a very simple approach, it is possible to predict the scattering and attenuation prop-

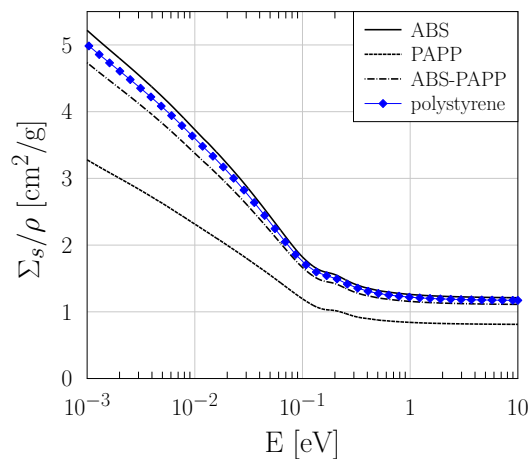


Figure 3. The mass attenuation coefficient for the polymer ABS based on the recipe from Ref.[23], compared with the one for polystyrene (blue triangles). The mass attenuation coefficient for PAPP and a mixture of ABS and PAPP are also reported as dashed and dotted-dashed lines, respectively.

erties of a vast family of materials so as to design suitable compounds for neutron applications in addition to the physical, mechanical, chemical and safety properties that are more often considered.

4 Outlook and Conclusions

We have provided a worked example on ABS to show how to calculate the total scattering cross section of polymers, especially 3D-printing materials, for thermal neutron energies and as a function of the sample temperature, simply taking into account the chemical physics of the material and using the Average Functional Group Approximation. This approach is available within NCrystal and, therefore, in several transport codes.

5 Acknowledgements

The authors gratefully acknowledge the support of the ISIS@MACH ITALIA Research Infrastructure, hub of ISIS Neutron and Muon Source (UK), [MUR Official Registry 0013837-04-08-2022]. The financial support from the Consiglio Nazionale delle Ricerche within the CNR-STFC Grant Agreement [No. 2021-2027] concerning collaboration in scientific research at the ISIS (UK) of STFC, is gratefully acknowledged.

References

- [1] MACFARLANE, R., MUIR, D.W., BOICOURT, R.M., KAHLER, III, A.C., AND CONLIN, J.L. The njoy nuclear data processing system, version 2016. *Los Alamos National Laboratory report LA-UR-17-20093* (2017).
- [2] Hawari A.I., Al-Qasir I.I., Gillette V.H., Wehring B.W. and Zhou T., *Proc. PHYSOR* **25**:25-9 (2004).
- [3] Damian J.M., Malaspina D.C. and Granada J.R., *The Journal of Chemical Physics* **139**(2), 024504 (2013).
- [4] Hawari A.I., *Nuclear Data Sheets*, **118**, 172-5 (2014).
- [5] Cai X.X. and Klinkby E., *New Journal of Physics*, **19**(10), 103027 (2017).
- [6] Wormald J. and Hawari A.I., *EPJ Web of Conferences* **146**, 13002 (2017).
- [7] Capelli S.C. and Romanelli G., *Journal of Applied Crystallography*, **52**(5), 1233-7 (2019)
- [8] Škoro G., Romanelli G., Rudic S., Lilley S., Fernandez-Alonso F., *EPJ Web of Conferences* **239**, 17008 (2020).
- [9] Cheng Y.Q. and Ramirez-Cuesta A.J., *Journal of Chemical Theory and Computation* **16**(8), 5212-7 (2020).
- [10] Cai, X.-X., and Kittelmann, T., *Computer Physics Communications*, **246**, 106851 (2020).
- [11] Laliena V., Dawidowski J., Cuello G.J. and Campo J., *Nucl. Instr. Meth. A*, **993**, 165071 (2021).
- [12] Romanelli G., Onorati D., Ulpiani P., Cancelli S., Perelli-Cippo E., Marquez Damian J. I., Capelli S. C., Croci G., Muraro A., Tardocchi M., Gorini G., *J. Phys.: Cond. Matt.* **33**(28), 285901 (2021).
- [13] Romanelli, G., Krzystyniak, M., Senesi, R., Raspino, D., Boxall, J., Pooley, D., Moorby, S., Schooneveld, E., Rhodes, N.J., Andreani, C. and Fernandez-Alonso, F., *Meas. Sci. Techn.*, **28**(9), p.095501 (2017).
- [14] Robledo J.I., Dawidowski J., Damián J.M., Škoro G., Bovo C., Romanelli G., *Nucl. Inst. Meth. A*, **971**, 164096 (2020).
- [15] Pietropaolo A., Andreani C., Filabozzi A., Senesi R., Gorini G., Perelli-Cippo E., Tardocchi M., Rhodes N.J., Schooneveld E.M., *J. Instr.* **1**(04), P04001, (2006)
- [16] Imberti S., Andreani C., Garbuio V., Gorini G., Pietropaolo A., Senesi R., Tardocchi M., *Nucl. Instr. and Meth.*, **552**, 463-476 (2005)
- [17] Witek, M., Krzystyniak, M., Romanelli, G., Witczak, T., *Polymers*, **13**(15), 2426 (2021).
- [18] Romanelli, G., Andreani, C., Fazi, L., Ishteev, A., Konstantinova, K., Preziosi, E., Di Carlo, A., *J. Chem. Phys.*, **157**(9), 094501 (2022).
- [19] Fernandez-Alonso F. and Price D.L., *Neutron Scattering* (Academic Press, 2013).
- [20] Sears V.F., *Neutron news* **3**(3), 26-37 (1992).
- [21] Ramić K., Damian J.I., Kittelmann T., Di Julio D.D., Campi D., Bernasconi M., Gorini G. and Santoro V., *Nucl. Inst. Meth. A*, **1027**, 166227 (2022).
- [22] <https://github.com/mctools/ncrystal/wiki/Data-library>, last accessed on October 2022.
- [23] Yuan, Z., Wen, H., Liu, Y., and Wang, Q., *Polymer Degradation and Stability*, **190**, 109639 (2021).
- [24] Ulpiani P., Romanelli G. Onorati D., Krzystyniak M., Andreani C., Senesi R., *J. Chem. Phys.*, **153**, 23, 234306 (2020).